

TECHNICAL REPORT

ISO/TR
15144-1

Second edition
2014-09-01

Calculation of micropitting load capacity of cylindrical spur and helical gears —

Part 1: Introduction and basic principles

Calcul de la capacité de charge aux micropiqûres des engrenages cylindriques à dentures droite et hélicoïdale —

Partie 1: Introduction et principes fondamentaux

STANDARDSISO.COM : Click to view the full PDF of ISO/TR 15144-1:2014



Reference number
ISO/TR 15144-1:2014(E)

© ISO 2014



COPYRIGHT PROTECTED DOCUMENT

© ISO 2014

All rights reserved. Unless otherwise specified, no part of this publication may be reproduced or utilized otherwise in any form or by any means, electronic or mechanical, including photocopying, or posting on the internet or an intranet, without prior written permission. Permission can be requested from either ISO at the address below or ISO's member body in the country of the requester.

ISO copyright office
Case postale 56 • CH-1211 Geneva 20
Tel. + 41 22 749 01 11
Fax + 41 22 749 09 47
E-mail copyright@iso.org
Web www.iso.org

Published in Switzerland

STANDARDSISO.COM : Click to view the full PDF of ISO/TR 15144-1:2014

Contents

	Page
Foreword	iv
Introduction	v
1 Scope	1
2 Normative references	1
3 Terms, definitions, symbols, and units	1
3.1 Terms and definitions	1
3.2 Symbols and units	2
4 Definition of micropitting	4
5 Basic formulae	5
5.1 General	5
5.2 Safety factor against micropitting, S_λ	5
5.3 Local specific lubricant film thickness, λ_{GFY}	6
5.4 Permissible specific lubricant film thickness, λ_{GFP}	7
5.5 Recommendation for the minimum safety factor against micropitting, $S_{\lambda,\min}$	7
6 Material parameter, G_M	8
6.1 Reduced modulus of elasticity, E_r	8
6.2 Pressure-viscosity coefficient at bulk temperature, $\alpha_{\theta M}$	9
7 Velocity parameter, U_Y	10
7.1 Sum of tangential velocities, $v_{\Sigma,Y}$	10
7.2 Dynamic viscosity at bulk temperature, $\eta_{\theta M}$	11
8 Load parameter, W_Y	12
8.1 Local Hertzian contact stress $p_{dyn,Y,A}$ according to Method A	12
8.2 Local Hertzian contact stress $p_{dyn,Y,B}$ according to Method B	12
9 Sliding parameter, S_{GFY}	13
9.1 Pressure-viscosity coefficient at local contact temperature, $\alpha_{\theta B,Y}$	14
9.2 Dynamic viscosity at local contact temperature, $\eta_{\theta B,Y}$	14
10 Definition of contact point Y on the path of contact	15
11 Load sharing factor, X_Y	17
11.1 Spur gears with unmodified profiles	18
11.2 Spur gears with profile modification	19
11.3 Buttressing factor, $X_{but,Y}$	20
11.4 Helical gears with $\varepsilon_\beta < 1$ and unmodified profiles	21
11.5 Helical gears with $\varepsilon_\beta < 1$ and profile modification	22
11.6 Helical gears with $\varepsilon_\beta \geq 1$ and unmodified profiles	23
11.7 Helical gears with $\varepsilon_\beta \geq 1$ and profile modification	23
12 Contact temperature, $\theta_{B,Y}$	25
13 Flash temperature, $\theta_{fl,Y}$	26
14 Bulk temperature, θ_M	26
14.1 Mean coefficient of friction, μ_m	27
14.2 Load losses factor, H_V	29
14.3 Tip relief factor, X_{Ca}	29
14.4 Lubrication factor, X_S	32
Annex A (informative) Calculation of the permissible specific lubricant film thickness λ_{GFP} for oils with a micropitting test result according to FVA-Information Sheet 54/7	33
Bibliography	35

Foreword

ISO (the International Organization for Standardization) is a worldwide federation of national standards bodies (ISO member bodies). The work of preparing International Standards is normally carried out through ISO technical committees. Each member body interested in a subject for which a technical committee has been established has the right to be represented on that committee. International organizations, governmental and non-governmental, in liaison with ISO, also take part in the work. ISO collaborates closely with the International Electrotechnical Commission (IEC) on all matters of electrotechnical standardization.

The procedures used to develop this document and those intended for its further maintenance are described in the ISO/IEC Directives, Part 1. In particular the different approval criteria needed for the different types of ISO documents should be noted. This document was drafted in accordance with the editorial rules of the ISO/IEC Directives, Part 2 (see www.iso.org/directives).

Attention is drawn to the possibility that some of the elements of this document may be the subject of patent rights. ISO shall not be held responsible for identifying any or all such patent rights. Details of any patent rights identified during the development of the document will be in the Introduction and/or on the ISO list of patent declarations received (see www.iso.org/patents).

Any trade name used in this document is information given for the convenience of users and does not constitute an endorsement.

For an explanation on the meaning of ISO specific terms and expressions related to conformity assessment, as well as information about ISO's adherence to the WTO principles in the Technical Barriers to Trade (TBT) see the following URL: Foreword - Supplementary information

The committee responsible for this document is ISO/TC 60, *Gears*, Subcommittee SC 2, *Gear capacity calculation*.

This second edition cancels and replaces the first edition (ISO/TR 15144-1:2010), which has been technically revised.

ISO/TR 15144 consists of the following parts, under the general title *Calculation of micropitting load capacity of cylindrical spur and helical gears*:

- *Part 1: Introduction and basic principles*
- *Part 2: Examples of calculation for micropitting*

Introduction

This part of ISO/TR 15144 provides principles for the calculation of the micropitting load capacity of cylindrical involute spur and helical gears with external teeth.

The basis for the calculation of the micropitting load capacity of a gear set is the model of the minimum operating specific lubricant film thickness in the contact zone. There are many influence parameters such as surface topology, contact stress level, and lubricant chemistry. While these parameters are known to affect the performance of micropitting for a gear set, the subject area remains a topic of research and, as such, the science has not yet developed to allow these specific parameters to be included directly in the calculation methods. Furthermore, the correct application of tip and root relief (involute modification) has been found to greatly influence micropitting; the suitable values should therefore be applied. Surface finish is another crucial parameter. At present, R_a is used but other aspects such as R_z or skewness have been observed to have significant effects which could be reflected in the finishing process applied.

Although the calculation of specific lubricant film thickness does not provide a direct method for assessing micropitting load capacity, it can serve as an evaluation criterion when applied as part of a suitable comparative procedure based on known gear performance.

STANDARDSISO.COM : Click to view the full PDF of ISO/TR 15144-1:2014

Calculation of micropitting load capacity of cylindrical spur and helical gears —

Part 1: Introduction and basic principles

1 Scope

This part of ISO/TR 15144 describes a procedure for the calculation of the micropitting load capacity of cylindrical gears with external teeth. It has been developed on the basis of testing and observation of oil-lubricated gear transmissions with modules between 3 mm and 11 mm and pitch line velocities of 8 m/s to 60 m/s. However, the procedure is applicable to any gear pair where suitable reference data are available, provided the criteria specified below are satisfied.

The formulae specified are applicable for driving, as well as for driven cylindrical gears with tooth profiles in accordance with the basic rack specified in ISO 53. They are also applicable for teeth conjugate to other basic racks where the virtual contact ratio is less than $\varepsilon_{\text{con}} = 2,5$. The results are in good agreement with other methods for normal working pressure angles up to 25°, reference helix angles up to 25°, and in cases where pitch line velocity is higher than 2 m/s.

This part of ISO/TR 15144 is not applicable for the assessment of types of gear tooth surface damage other than micropitting.

2 Normative references

The following documents, in whole or in part, are normatively referenced in this document and are indispensable for its application. For dated references, only the edition cited applies. For undated references, the latest edition of the referenced document (including any amendments) applies.

ISO 53, *Cylindrical gears for general and heavy engineering — Standard basic rack tooth profile*

ISO 1122-1, *Vocabulary of gear terms — Part 1: Definitions related to geometry*

ISO 1328-1, *Cylindrical gears — ISO system of flank tolerance classification — Part 1: Definitions and allowable values of deviations relevant to flanks of gear teeth*

ISO 6336-1, *Calculation of load capacity of spur and helical gears — Part 1: Basic principles, introduction and general influence factors*

ISO 6336-2, *Calculation of load capacity of spur and helical gears — Part 2: Calculation of surface durability (pitting)*

3 Terms, definitions, symbols, and units

3.1 Terms and definitions

For the purposes of this document, the terms and definitions given in ISO 1122-1, ISO 6336-1, and ISO 6336-2 apply.

3.2 Symbols and units

The symbols used in ISO/TR 15144 are given in [Table 1](#). The units of length metre, millimetre, and micrometre are chosen in accordance with common practice. The conversions of the units are already included in the given equations.

Table 1 — Symbols and units

Symbol	Description	Unit
a	centre distance	mm
B_{M1}	thermal contact coefficient of pinion	N/(m·s ^{0.5} ·K)
B_{M2}	thermal contact coefficient of wheel	N/(m·s ^{0.5} ·K)
b	face width	mm
c_{a1}	tip relief of pinion	µm
c_{a2}	tip relief of wheel	µm
c_{eff}	effective tip relief	µm
c_{M1}	specific heat per unit mass of pinion	J/(kg·K)
c_{M2}	specific heat per unit mass of wheel	J/(kg·K)
c'	maximum tooth stiffness per unit face width (single stiffness) of a tooth pair	N/(mm·µm)
$c_{\gamma\alpha}$	mean value of mesh stiffness per unit face width	N/(mm·µm)
d_{a1}	tip diameter of pinion	mm
d_{a2}	tip diameter of wheel	mm
d_{b1}	base diameter of pinion	mm
d_{b2}	base diameter of wheel	mm
d_{w1}	pitch diameter of pinion	mm
d_{w2}	pitch diameter of wheel	mm
d_{Y1}	Y-circle diameter of pinion	mm
d_{Y2}	Y-circle diameter of wheel	mm
E_r	reduced modulus of elasticity	N/mm ²
E_1	modulus of elasticity of pinion	N/mm ²
E_2	modulus of elasticity of wheel	N/mm ²
F_{bt}	nominal transverse load in plane of action (base tangent plane)	N
F_t	(nominal) transverse tangential load at reference cylinder per mesh	N
G_M	material parameter	—
g_Y	parameter on the path of contact (distance of point Y from point A)	mm
g_α	length of path of contact	mm
H_v	load losses factor	—
h_Y	local lubricant film thickness	µm
K_A	application factor	—
$K_{H\alpha}$	transverse load factor	—
$K_{H\beta}$	face load factor	—
K_v	dynamic factor	—
n_1	rotation speed of pinion	min ⁻¹
P	transmitted power	kW
p_{et}	transverse base pitch on the path of contact	mm

Table 1 (continued)

Symbol	Description	Unit
$p_{\text{dyn},Y}$	local Hertzian contact stress including the load factors K	N/mm ²
$p_{\text{H},Y}$	local nominal Hertzian contact stress	N/mm ²
R_a	effective arithmetic mean roughness value	µm
R_{a1}	arithmetic mean roughness value of pinion	µm
R_{a2}	arithmetic mean roughness value of wheel	µm
$S_{\text{GF},Y}$	local sliding parameter	—
S_λ	safety factor against micropitting	—
$S_{\lambda,\text{min}}$	minimum required safety factor against micropitting	—
T_1	nominal torque at the pinion	Nm
U_Y	local velocity parameter	—
u	gear ratio	—
$v_{g,Y}$	local sliding velocity	m/s
VI	viscosity improver	—
$v_{r1,Y}$	local tangential velocity on pinion	m/s
$v_{r2,Y}$	local tangential velocity on wheel	m/s
$v_{\Sigma,C}$	sum of tangential velocities at pitch point	m/s
$v_{\Sigma,Y}$	sum of tangential velocities at point Y	m/s
W_w	material factor	—
W_Y	local load parameter	—
$X_{\text{but},Y}$	local buttressing factor	—
X_{Ca}	tip relief factor	—
X_L	lubricant factor	—
X_R	roughness factor	—
X_S	lubrication factor	—
X_Y	local load sharing factor	—
Z_E	elasticity factor	(N/mm ²) ^{0,5}
z_1	number of teeth of pinion	—
z_2	number of teeth of wheel	—
α_t	transverse pressure angle	°
α_{wt}	pressure angle at the pitch cylinder	°
$\alpha_{\theta B,Y}$	pressure-viscosity coefficient at local contact temperature	m ² /N
$\alpha_{\theta M}$	pressure-viscosity coefficient at bulk temperature	m ² /N
α_{38}	pressure-viscosity coefficient at 38 °C	m ² /N
β_b	base helix angle	°
ε_{max}	maximum addendum contact ratio	—
ε_α	transverse contact ratio	—
ε_{an}	virtual contact ratio, transverse contact ratio of a virtual spur gear	—
ε_β	overlap ratio	—
ε_γ	total contact ratio	—
ε_1	addendum contact ratio of the pinion	—
ε_2	addendum contact ratio of the wheel	—

Table 1 (continued)

Symbol	Description	Unit
$\eta_{\theta B,Y}$	dynamic viscosity at local contact temperature	N·s/m ²
$\eta_{\theta M}$	dynamic viscosity at bulk temperature	N·s/m ²
$\eta_{\theta oil}$	dynamic viscosity at oil inlet/sump temperature	N·s/m ²
η_{38}	dynamic viscosity at 38 °C	N·s/m ²
$\theta_{B,Y}$	local contact temperature	°C
$\theta_{fl,Y}$	local flash temperature	°C
θ_M	bulk temperature	°C
θ_{oil}	oil inlet/sump temperature	°C
$\lambda_{GF,min}$	minimum specific lubricant film thickness in the contact area	—
$\lambda_{GF,Y}$	local specific lubricant film thickness	—
λ_{GFP}	permissible specific lubricant film thickness	—
λ_{GFT}	limiting specific lubricant film thickness of the test gears	—
λ_{M1}	specific heat conductivity of pinion	W/(m·K)
λ_{M2}	specific heat conductivity of wheel	W/(m·K)
μ_m	mean coefficient of friction	—
$\nu_{\theta B,Y}$	kinematic viscosity at local contact temperature	mm ² /s
$\nu_{\theta M}$	kinematic viscosity at bulk temperature	mm ² /s
ν_1	Poisson's ratio of pinion	—
ν_2	Poisson's ratio of wheel	—
ν_{100}	kinematic viscosity at 100 °C	mm ² /s
ν_{40}	kinematic viscosity at 40 °C	mm ² /s
ρ_{M1}	density of pinion	kg/m ³
ρ_{M2}	density of wheel	kg/m ³
$\rho_{n,C}$	normal radius of relative curvature at pitch diameter	mm
$\rho_{n,Y}$	normal radius of relative curvature at point Y	mm
$\rho_{t,Y}$	transverse radius of relative curvature at point Y	mm
$\rho_{t1,Y}$	transverse radius of curvature of pinion at point Y	mm
$\rho_{t2,Y}$	transverse radius of curvature of wheel at point Y	mm
$\rho_{\theta B,Y}$	density of lubricant at local contact temperature	kg/m ³
$\rho_{\theta M}$	density of lubricant at bulk temperature	kg/m ³
ρ_{15}	density of lubricant at 15 °C	kg/m ³
Subscripts to symbols		
Y	Parameter for any contact point Y in the contact area for method A and on the path of contact for method B; (all parameters subscript Y have to be calculated with local values)	

4 Definition of micropitting

Micropitting is a phenomenon that occurs in Hertzian type of rolling and sliding contact that operates in elastohydrodynamic or boundary lubrication regimes. Micropitting is influenced by operating conditions such as load, speed, sliding, temperature, surface topography, specific lubricant film thickness, and chemical composition of the lubricant. Micropitting is more commonly observed on materials with a high surface hardness.

Micropitting is the generation of numerous surface cracks. The cracks grow at a shallow angle to the surface forming micropits. The micropits are small relative to the size of the contact zone, typically of the order 10 µm–20 µm deep. The micropits can coalesce to produce a continuous fractured surface which appears as a dull, matte surface during unmagnified visual inspection.

Micropitting is the preferred name for this phenomenon, but it has also been referred to as grey staining, grey flecking, frosting, and peeling. Illustrations of micropitting can be found in ISO 10825.

Micropitting can arrest. However, if micropitting continues to progress, it can result in reduced gear tooth accuracy, increased dynamic loads, and noise. If it does not arrest and continues to propagate, it can develop into macropitting and other modes of gear failure.

5 Basic formulae

5.1 General

The calculation of micropitting load capacity is based on the local specific lubricant film thickness $\lambda_{GF,Y}$ in the contact area and the permissible specific lubricant film thickness λ_{GFP} .^[10] It is assumed that micropitting can occur when the minimum specific lubricant film thickness $\lambda_{GF,min}$ is lower than a corresponding critical value λ_{GFP} . Both values $\lambda_{GF,min}$ and λ_{GFP} shall be calculated separately for pinion and wheel in the contact area. It has to be recognized that the determination of the minimum specific lubricant film thickness and the permissible specific lubricant film thickness have to be based on the operating parameters.

The micropitting load capacity can be determined by comparing the minimum specific lubricant film thickness with the corresponding limiting value derived from gears in service or from specific gear testing. This comparison will be expressed by the safety factor S_λ which shall be equal or higher than a minimum safety factor against micropitting $S_{\lambda,min}$.

Micropitting mainly occurs in areas of negative specific sliding. Negative specific sliding is to be found along the path of contact (see [Figure 1](#)) between points A and C on the driving gear and between points C and E on the driven gear. Considering the influences of lubricant, surface roughness, geometry of the gears, and operating conditions, the specific lubricant film thickness $\lambda_{GF,Y}$ can be calculated for every point in the field of contact.

5.2 Safety factor against micropitting, S_λ

To account for the micropitting load capacity, the safety factor S_λ according to Formula (1) is defined.

$$S_\lambda = \frac{\lambda_{GF,min}}{\lambda_{GFP}} \geq S_{\lambda,min} \quad (1)$$

where

- $\lambda_{GF,min} = \min (\lambda_{GF,Y})$ is the minimum specific lubricant film thickness in the contact area;
- $\lambda_{GF,Y}$ is the local specific lubricant film thickness (see [5.3](#));
- λ_{GFP} is the permissible specific lubricant film thickness (see [5.4](#));
- $S_{\lambda,min}$ is the minimum required safety factor (see [5.5](#)).

The minimum specific lubricant film thickness is determined from all calculated local values of the specific lubricant film thickness $\lambda_{GF,Y}$ obtained by Formula (2).

5.3 Local specific lubricant film thickness, $\lambda_{GF,Y}$

For the determination of the safety factor S_λ , the local lubricant film thickness h_Y according to Dowson/Higginson^[5] in the field of contact has to be known and compared with the effective surface roughness.

$$\lambda_{GF,Y} = \frac{h_Y}{Ra} \quad (2)$$

where

$$Ra = 0,5 \cdot (Ra_1 + Ra_2) \quad (3)$$

$$h_Y = 1600 \cdot \rho_{n,Y} \cdot G_M^{0,6} \cdot U_Y^{0,7} \cdot W_Y^{-0,13} \cdot S_{GF,Y}^{0,22} \quad (4)$$

Ra is the effective arithmetic mean roughness value;

Ra_1 is the arithmetic mean roughness value of pinion (compare ISO 6336-2);

Ra_2 is the arithmetic mean roughness value of wheel (compare ISO 6336-2);

h_Y is the local lubricant film thickness;

$\rho_{n,Y}$ is the normal radius of relative curvature at point Y (see [Clause 10](#));

G_M is the material parameter (see [Clause 6](#));

U_Y is the local velocity parameter (see [Clause 7](#));

W_Y is the local load parameter (see [Clause 8](#));

$S_{GF,Y}$ is the local sliding parameter (see [Clause 9](#)).

Formula (4) should be calculated in the case of Method B at the seven local points (Y) defined in [5.3 b\)](#) using the values for $\rho_{n,Y}$, U_Y , W_Y , and $S_{GF,Y}$ that exists at each point Y. The minimum of the seven h_Y ($\lambda_{GF,Y}$) values shall be used in Formula (1).

Example calculations are presented in ISO/TR 15144-2.

a) Method A

The local specific lubricant film thickness can be determined in the complete contact area by any appropriate gear computing program. In order to determine the local specific lubricant film thickness, the load distribution, the influence of normal and sliding velocity with changes of meshing phase, and the actual service conditions shall be taken into consideration.

b) Method B

This method involves the assumption that the determinant local specific lubricant film thickness occurs on the tooth flank in the area of negative sliding. For simplification, the calculation of the local specific lubricant film thickness is limited to certain points on the path of contact. For this purpose, the lower point A and upper point E on the path of contact, the lower point B and upper point D of single pair tooth contact, the midway point AB between A and B, the midway point DE between D and E, as well as the pitch point C, are surveyed. Furthermore, for the calculation, two cases are differentiated: case 1 – no profile modification, case 2 – adequate profile modification according to manufacturers' experience. In case of profile modifications, lower than adequate profile modifications, case 1 has to be used. In case of too high profile modifications it is recommended to use Method A.

5.4 Permissible specific lubricant film thickness, λ_{GFP}

For the determination of the permissible specific lubricant film thickness λ_{GFP} , different procedures are applicable.

a) Method A

For Method A, experimental investigations or service experience relating to micropitting on real gears are used.

Running real gears under conditions where micropitting just occurs, the minimum specific lubricant film thickness can be calculated according to [5.3 a\)](#). This value is equivalent to the limiting specific lubricant film thickness which is used to calculate the micropitting load capacity.

Such experimental investigations can be performed on gears having the same design as the actual gear pair. In this case, the gear manufacturing, gear accuracy, operating conditions, lubricant, and operating temperature have to be appropriate for the actual gear box.

The cost required for this method is, in general, only justifiable for the development of new products, as well as for gear boxes where failure would have serious consequences.

Otherwise, the permissible specific lubricant film thickness λ_{GFP} can be derived from consideration of dimensions, service conditions, and performance of carefully monitored reference gears operated with the respective lubricant. The more closely the dimensions and service conditions of the actual gears resemble those of the reference gears, the more effective will be the application of such values for the purpose of design ratings or calculation checks.

b) Method B

The method adapted is validated by carrying out careful comparative studies of well-documented histories of a number of test gears applicable to the type, quality, and manufacture of gearing under consideration. The permissible specific lubricant film thickness λ_{GFP} is calculated from the critical specific lubricant film thickness λ_{GFT} which is the result of any standardised test method applicable to evaluate the micropitting load capacity of lubricants or materials by means of defined test gears operated under specified test conditions. λ_{GFT} is a function of the temperature, oil viscosity, base oil, and additive chemistry and can be calculated according to Formula (2) in the contact point of the defined test gears where the minimum specific lubricant film thickness is to be found and for the test conditions where the failure limit concerning micropitting in the standardised test procedure has been reached.

The test gears, as well as the test conditions (for example, the test temperature), have to be appropriate for the real gears in consideration.

Any standardised test can be used to determine the data. Where a specific test procedure is not available or required, a number of internationally available standardised test methods for the evaluation of micropitting performance of gears, lubricants, and materials are currently available. Some widely used test procedures are the FVA-FZG-micropitting test,[\[7\]](#) Flender micropitting test,[\[11\]](#) BGA-DU micropitting test,[\[2\]](#) and the micropitting test according to Reference [\[3\]](#). [Annex A](#) provides some generalized test data (for reference only) that have been produced using the test procedure according to FVA-Information Sheet 54/7[\[2\]](#) where a value for λ_{GFP} can be calculated for a generalized reference allowable using Formula (A.1).

5.5 Recommendation for the minimum safety factor against micropitting, $S_{\lambda, \min}$

For a given application, adequate micropitting load capacity is demonstrated by the computed value of S_{λ} and being greater than or equal to the value $S_{\lambda, \min}$, respectively.

Certain minimum values for the safety factor shall be determined. Recommendations concerning these minimum values are made in the following, but values are not proposed.

An appropriate probability of failure and the safety factor shall be carefully chosen to meet the required reliability at a justifiable cost. If the performance of the gears can be accurately appraised through

testing of the actual unit under actual load conditions, a lower safety factor and more economical manufacturing procedures may be permissible:

$$\text{Safety factor} = \frac{\text{Calculated minimum specific film thickness}}{\text{Permissible specific film thickness}}$$

In addition to the general requirements mentioned and the special requirements for specific lubricant film thickness, the safety factor shall be chosen after careful consideration of the following influences.

- Reliability of load values used for calculation: If loads or the response of the system to vibration are estimated rather than measured, a larger safety factor should be used;
- Variations in gear geometry and surface texture due to manufacturing tolerances;
- Variations in alignment;
- variations in material due to process variations in chemistry, cleanliness, and microstructure (material quality and heat treatment);
- Variations in lubrication and its maintenance over the service life of the gears.

Depending on the reliability of the assumptions on which the calculations are based (for example, load assumptions) and according to the reliability requirements (consequences of occurrence), a corresponding safety factor is to be chosen.

Where gears are produced according to a specification or a request for proposal (quotation), in which the gear supplier is to provide gears or assembled gear drives having specified calculated capacities (ratings) in accordance with this technical report, the value of the safety factor for micropitting is to be agreed upon between the parties.

6 Material parameter, G_M

The material parameter, G_M , accounts for the influence of the reduced modulus of elasticity, E_r , and the pressure-viscosity coefficient of the lubricant at bulk temperature, $\alpha_{\theta M}$.

$$G_M = 10^6 \cdot \alpha_{\theta M} \cdot E_r \quad (5)$$

where

E_r is the reduced modulus of elasticity (see [6.1](#));

$\alpha_{\theta M}$ is the pressure-viscosity coefficient at bulk temperature (see [6.2](#)).

6.1 Reduced modulus of elasticity, E_r

For mating gears of different material and modulus of elasticity E_1 and E_2 , the reduced modulus of elasticity, E_r , can be determined by Formula (6). For mating gears of the same material $E = E_1 = E_2$, Formula (7) can be used.

$$E_r = 2 \cdot \left(\frac{1 - v_1^2}{E_1} + \frac{1 - v_2^2}{E_2} \right)^{-1} \quad (6)$$

$$E_r = \frac{E}{1-v^2} \quad \text{for } E_1 = E_2 = E \text{ and } v_1 = v_2 = v \quad (7)$$

where

E_1 is the modulus of elasticity of pinion (for steel: $E = 206000 \text{ N/mm}^2$);

E_2 is the modulus of elasticity of wheel (for steel: $E = 206000 \text{ N/mm}^2$);

v_1 is the Poisson's ratio of pinion (for steel: $v = 0,3$);

v_2 is the Poisson's ratio of wheel (for steel: $v = 0,3$).

6.2 Pressure-viscosity coefficient at bulk temperature, $\alpha_{\theta M}$

If the data for the pressure-viscosity coefficient at bulk temperature $\alpha_{\theta M}$ for the specific lubricant is not available, it can be approximated by Formula (8). See Reference [8].

$$\alpha_{\theta M} = \alpha_{38} \cdot \left[1 + 516 \cdot \left(\frac{1}{\theta_M + 273} - \frac{1}{311} \right) \right] \quad (8)$$

where

α_{38} is the pressure-viscosity coefficient of the lubricant at 38 °C;

θ_M is the bulk temperature (see [Clause 14](#)).

If no values for α_{38} are available then the following approximated values^[1] can be used.

$$\alpha_{38} = 2,657 \cdot 10^{-8} \cdot \eta_{38}^{0,1348} \quad \text{for mineral oil} \quad (9)$$

$$\alpha_{38} = 1,466 \cdot 10^{-8} \cdot \eta_{38}^{0,0507} \quad \text{for PAO - based synthetic non-VI improved oil} \quad (10)$$

$$\alpha_{38} = 1,392 \cdot 10^{-8} \cdot \eta_{38}^{0,1572} \quad \text{for PAG - based synthetic oil} \quad (11)$$

where

η_{38} is the dynamic viscosity of the lubricant at 38 °C.

7 Velocity parameter, U_Y

The velocity parameter U_Y describes the proportional increase of the specific lubricant film thickness with increasing dynamic viscosity $\eta_{\theta M}$ of the lubricant at bulk temperature and sum of the tangential velocities $v_{\Sigma,Y}$.

$$U_Y = \eta_{\theta M} \cdot \frac{v_{\Sigma,Y}}{2000 \cdot E_r \cdot p_{n,Y}} \quad (12)$$

where

$\eta_{\theta M}$ is the dynamic viscosity of the lubricant at bulk temperature (see 7.2);

$v_{\Sigma,Y}$ is the sum of the tangential velocities (see 7.1);

E_r is the reduced modulus of elasticity (see 6.1);

$p_{n,Y}$ is the local normal radius of relative curvature (see Clause 10).

7.1 Sum of tangential velocities, $v_{\Sigma,Y}$

The sum of the tangential velocities at a mesh point Y is calculated according to Formula (13). The velocity for pinion, $v_{r1,Y}$, and wheel, $v_{r2,Y}$, in a certain contact point Y on the tooth flank depends on the diameter at pinion, d_{Y1} , and the diameter at wheel d_{Y2} of point Y.

$$v_{\Sigma,Y} = v_{r1,Y} + v_{r2,Y} \quad (13)$$

where

$$v_{r1,Y} = 2 \cdot \pi \cdot \frac{n_1}{60} \cdot \frac{d_{w1}}{2000} \cdot \sin \alpha_{wt} \cdot \sqrt{\frac{d_{Y1}^2 - d_{b1}^2}{d_{w1}^2 - d_{b1}^2}} \quad (14)$$

$$v_{r2,Y} = 2 \cdot \pi \cdot \frac{n_1}{u \cdot 60} \cdot \frac{d_{w2}}{2000} \cdot \sin \alpha_{wt} \cdot \sqrt{\frac{d_{Y2}^2 - d_{b2}^2}{d_{w2}^2 - d_{b2}^2}} \quad (15)$$

$v_{r1,Y}$ is the tangential velocity on pinion (see Figure 1);

$v_{r2,Y}$ is the tangential velocity on wheel (see Figure 1);

d_{b1} is the base diameter of pinion;

d_{b2} is the base diameter of wheel;

d_{w1} is the pitch diameter of pinion;

d_{w2} is the pitch diameter of wheel;

d_{Y1} is the Y-circle diameter of pinion (see Figure 1 and Clause 10);

d_{Y2} is the Y-circle diameter of wheel (see Figure 1 and Clause 10);

n_1 is the rotation speed of pinion;

$u = z_2/z_1$ is the gear ratio;

α_{wt} is the pressure angle at the pitch cylinder.

7.2 Dynamic viscosity at bulk temperature, η_{0M}

The dynamic viscosity at bulk temperature η_{0M} can be calculated according to Formula (16).

$$\eta_{0M} = 10^{-6} \cdot \nu_{0M} \cdot \rho_{0M} \quad (16)$$

where

ν_{0M} is the kinematic viscosity of the lubricant at bulk temperature (see [7.2.1](#));

ρ_{0M} is the density of the lubricant at bulk temperature (see [7.2.2](#)).

7.2.1 Kinematic viscosity at bulk temperature, ν_{0M}

The kinematic viscosity at bulk temperature, ν_{0M} , can be calculated from the kinematic viscosity ν_{40} at 40 °C and the kinematic viscosity ν_{100} at 100 °C on the basis of Formula (17). Extrapolation for temperature higher than 140 °C should be confirmed by measurement.

$$\log[\log(\nu_{0M} + 0,7)] = A \cdot \log(\theta_M + 273) + B \quad (17)$$

where

$$A = \frac{\log[\log(\nu_{40} + 0,7) / \log(\nu_{100} + 0,7)]}{\log(313 / 373)} \quad (18)$$

$$B = \log[\log(\nu_{40} + 0,7)] - A \cdot \log(313) \quad (19)$$

θ_M is the bulk temperature (see [Clause 14](#));

ν_{40} is the kinematic viscosity of the lubricant at 40 °C;

ν_{100} is the kinematic viscosity of the lubricant at 100 °C.

7.2.2 Density of the lubricant at bulk temperature, ρ_{0M}

If the density of the lubricant at bulk temperature ρ_{0M} is not available, it can be approximated based on the density of the lubricant at 15 °C according to Formula (20).

$$\rho_{0M} = \rho_{15} \cdot \left[1 - 0,7 \cdot \frac{(\theta_M + 273) - 289}{\rho_{15}} \right] \quad (20)$$

where

ρ_{15} is the density of the lubricant at 15 °C according to the lubricant data sheet;

θ_M is the bulk temperature (see [Clause 14](#)).

If no data for ρ_{15} is available, then Formula (21) can be used for approximation of mineral oils.

$$\rho_{15} = 43,37 \cdot \log \nu_{40} + 805,5 \quad (21)$$

ν_{40} is the kinematic viscosity of the lubricant at 40 °C.

8 Load parameter, W_Y

The load parameter W_Y can be determined using the local Hertzian contact stress $p_{\text{dyn},Y}$ and the reduced modulus of elasticity E_r .

$$W_Y = \frac{2 \cdot \pi \cdot p_{\text{dyn},Y}^2}{E_r^2} \quad (22)$$

where

$p_{\text{dyn},Y}$ is the local Hertzian contact stress according to Method A (see 8.1) or according to Method B (see 8.2);

E_r is the reduced modulus of elasticity (see 6.1).

8.1 Local Hertzian contact stress $p_{\text{dyn},Y,A}$ according to Method A

The local Hertzian contact stress $p_{\text{dyn},Y,A}$, according to Method A, should be determined by means of a 3D mesh contact and load distribution analysis procedure. The local nominal Hertzian contact stress determined from the elastic mesh contact model $p_{H,Y,A}$ is applied to Formula (23) to obtain the local Hertzian contact stress $p_{\text{dyn},Y,A}$.

$$p_{\text{dyn},Y,A} = p_{H,Y,A} \cdot \sqrt{K_A \cdot K_v} \quad (23)$$

where

$p_{H,Y,A}$ is the local nominal Hertzian contact stress, calculated with a 3D load distribution program;

K_A is the application factor (according to ISO 6336-1);

K_v is the dynamic factor (according to ISO 6336-1).

NOTE Where either K_A or K_v influences are already considered in the 3D elastic mesh contact model, either or both K_A and K_v should be set as 1.0 in Formula (23).

8.2 Local Hertzian contact stress $p_{\text{dyn},Y,B}$ according to Method B

The local Hertzian contact stress $p_{\text{dyn},Y,B}$, according to Method B, is calculated according to Formula (24). The required nominal Hertzian contact stress $p_{H,Y,B}$ is obtained by Formula (25), see 8.2.1. The total load in the case of drive trains with multiple transmission paths or planetary gear systems is not quite evenly distributed over the individual meshes. This is to be taken into consideration by inserting a distribution factor K_Y to follow K_A in Formula (24), to adjust the average load per mesh as necessary.

$$p_{\text{dyn},Y,B} = p_{H,Y,B} \cdot \sqrt{K_A \cdot K_v \cdot K_{H\alpha} \cdot K_{H\beta}} \quad (24)$$

where

- $p_{H,Y,B}$ is the local nominal Hertzian contact stress (see 8.2.1);
- K_A is the application factor (according to ISO 6336-1);
- K_v is the dynamic factor (according to ISO 6336-1);
- $K_{H\alpha}$ is the transverse load factor (according to ISO 6336-1) [profile modifications are considered in the factor X_Y (see [Clause 11](#))];
- $K_{H\beta}$ is the face load factor (according to ISO 6336-1) (lead modifications are considered in this factor).

NOTE Gears with a transverse contact ratio $\varepsilon_\alpha > 2$ can only be calculated according to Method A.

8.2.1 Nominal Hertzian contact stress $p_{H,Y,B}$

The nominal Hertzian contact stress $p_{H,Y,B}$ is used to determine the local Hertzian contact stress $p_{dyn,Y,B}$ (see [8.1](#)). To take the influence of different profile modifications into account, the load sharing factor X_Y is introduced. For the calculation of the local nominal Hertzian contact stress, the local nominal radius of relative curvature is used.

$$p_{H,Y,B} = Z_E \cdot \sqrt{\frac{F_t \cdot X_Y}{b \cdot \rho_{n,Y} \cdot \cos \alpha_t \cdot \cos \beta_b}} \quad (25)$$

where

$$Z_E = \sqrt{\frac{E_r}{2\pi}} \quad (26)$$

- Z_E is the elasticity factor (according to ISO 6336-2);
- b is the face width;
- F_t is the transverse tangential load at reference cylinder;
- X_Y is the load sharing factor (see [Clause 11](#));
- E_r is the reduced modulus of elasticity (see [6.1](#));
- α_t is the transverse pressure angle;
- β_b is the base helix angle;
- $\rho_{n,Y}$ is the local normal radius of relative curvature (see [Clause 10](#)).

9 Sliding parameter, S_{GFY}

The sliding parameter S_{GFY} accounts for the influence of local sliding on the local temperature. This temperature influences both the local pressure-viscosity coefficient and the local dynamic viscosity and hence the local lubricant film thickness.[\[6\]](#) The indices “ $\theta_{B,Y}$ ” for local contact temperature and “ θ_M ” for

bulk temperature are used. The local contact temperature $\theta_{B,Y}$ is the sum of the local flash $\theta_{fl,Y}$ and the bulk temperature θ_M .

$$S_{GF,Y} = \frac{\alpha_{\theta_{B,Y}} \cdot \eta_{\theta_{B,Y}}}{\alpha_{\theta_M} \cdot \eta_{\theta_M}} \quad (27)$$

where

$\alpha_{\theta_{B,Y}}$ is the pressure-viscosity coefficient at local contact temperature (see 9.1);

$\eta_{\theta_{B,Y}}$ is the dynamic viscosity at local contact temperature (see 9.2);

α_{θ_M} is the pressure-viscosity coefficient at bulk temperature (see 6.2);

η_{θ_M} is the dynamic viscosity at bulk temperature (see 7.2).

9.1 Pressure-viscosity coefficient at local contact temperature, $\alpha_{\theta_{B,Y}}$

If the data for the pressure-viscosity coefficient at local contact temperature $\alpha_{\theta_{B,Y}}$ for the specific lubricant is not available, it can be approximated by Formula (28). See Reference [8].

$$\alpha_{\theta_{B,Y}} = \alpha_{38} \cdot \left[1 + 516 \cdot \left(\frac{1}{\theta_{B,Y} + 273} - \frac{1}{311} \right) \right] \quad (28)$$

where

α_{38} is the pressure-viscosity coefficient of the lubricant at 38 °C (see also 6.2);

$\theta_{B,Y}$ is the local contact temperature (see Clause 12).

9.2 Dynamic viscosity at local contact temperature, $\eta_{\theta_{B,Y}}$

The dynamic viscosity at local contact temperature, $\eta_{\theta_{B,Y}}$, is determined by Formula (29).

$$\eta_{\theta_{B,Y}} = 10^{-6} \cdot \nu_{\theta_{B,Y}} \cdot \rho_{\theta_{B,Y}} \quad (29)$$

where

$\nu_{\theta_{B,Y}}$ is the kinematic viscosity at local contact temperature (see 9.2.1);

$\rho_{\theta_{B,Y}}$ is the density of the lubricant at local contact temperature (see 9.2.2).

9.2.1 Kinematic viscosity at local contact temperature $\nu_{\theta_{B,Y}}$

The kinematic viscosity at local contact temperature $\nu_{\theta_{B,Y}}$ can be calculated from the kinematic viscosity ν_{40} at 40 °C and the kinematic viscosity ν_{100} at 100 °C on the basis of Formula (30). Extrapolation for temperature higher than 140 °C should be confirmed by measurement.

$$\log[\log(\nu_{\theta_{B,Y}} + 0,7)] = A \cdot \log(\theta_{B,Y} + 273) + B \quad (30)$$

where

$$A = \frac{\log[\log(\nu_{40} + 0,7) / \log(\nu_{100} + 0,7)]}{\log(313 / 373)} \quad (31)$$

$$B = \log[\log(\nu_{40} + 0,7)] - A \cdot \log(313) \quad (32)$$

$\theta_{B,Y}$ is the local contact temperature (see [Clause 12](#));

ν_{40} is the kinematic viscosity of the lubricant at 40 °C;

ν_{100} is the kinematic viscosity of the lubricant at 100 °C.

9.2.2 Density of the lubricant at local contact temperature $\rho_{\theta B,Y}$

If the density of the lubricant at local contact temperature $\rho_{\theta B,Y}$ is not available, it can be approximated based on the density of the lubricant at 15 °C according to Formula (33).

$$\rho_{\theta B,Y} = \rho_{15} \cdot \left[1 - 0,7 \cdot \frac{(\theta_{B,Y} + 273) - 289}{\rho_{15}} \right] \quad (33)$$

where

ρ_{15} is the density of the lubricant at 15 °C according to the lubricant data sheet (see also [7.2.2](#));

$\theta_{B,Y}$ is the local contact temperature (see [Clause 12](#)).

10 Definition of contact point Y on the path of contact

Contact point Y is located between the SAP (contact point A) and EAP (contact point E) on the path of contact according to [Figure 1](#). It describes the actual contact point between pinion and wheel in a certain meshing position g_Y .

According to [5.3](#) Method B, the calculation has to be done for the following contact points:

Y =

A $g_Y = g_A = 0 \text{ mm}$ the lower point on the path of contact (34)

AB $g_Y = g_{AB} = (g_\alpha - p_{et}) / 2$ the midway point between A and B (35)

B $g_Y = g_B = g_\alpha - p_{et}$ the lower point of single pair tooth contact (36)

C $g_Y = g_C = \frac{d_{b1}}{2} \cdot \tan \alpha_{wt} - \sqrt{\frac{d_{a1}^2}{4} - \frac{d_{b1}^2}{4}} + g_\alpha$ the pitch point (37)

D $g_Y = g_D = p_{et}$ the upper point of single pair tooth contact (38)

DE $g_Y = g_{DE} = (g_\alpha - p_{et}) / 2 + p_{et}$ the midway point between D and E (39)

E $g_Y = g_E = g_\alpha$ the upper point on the path of contact (40)

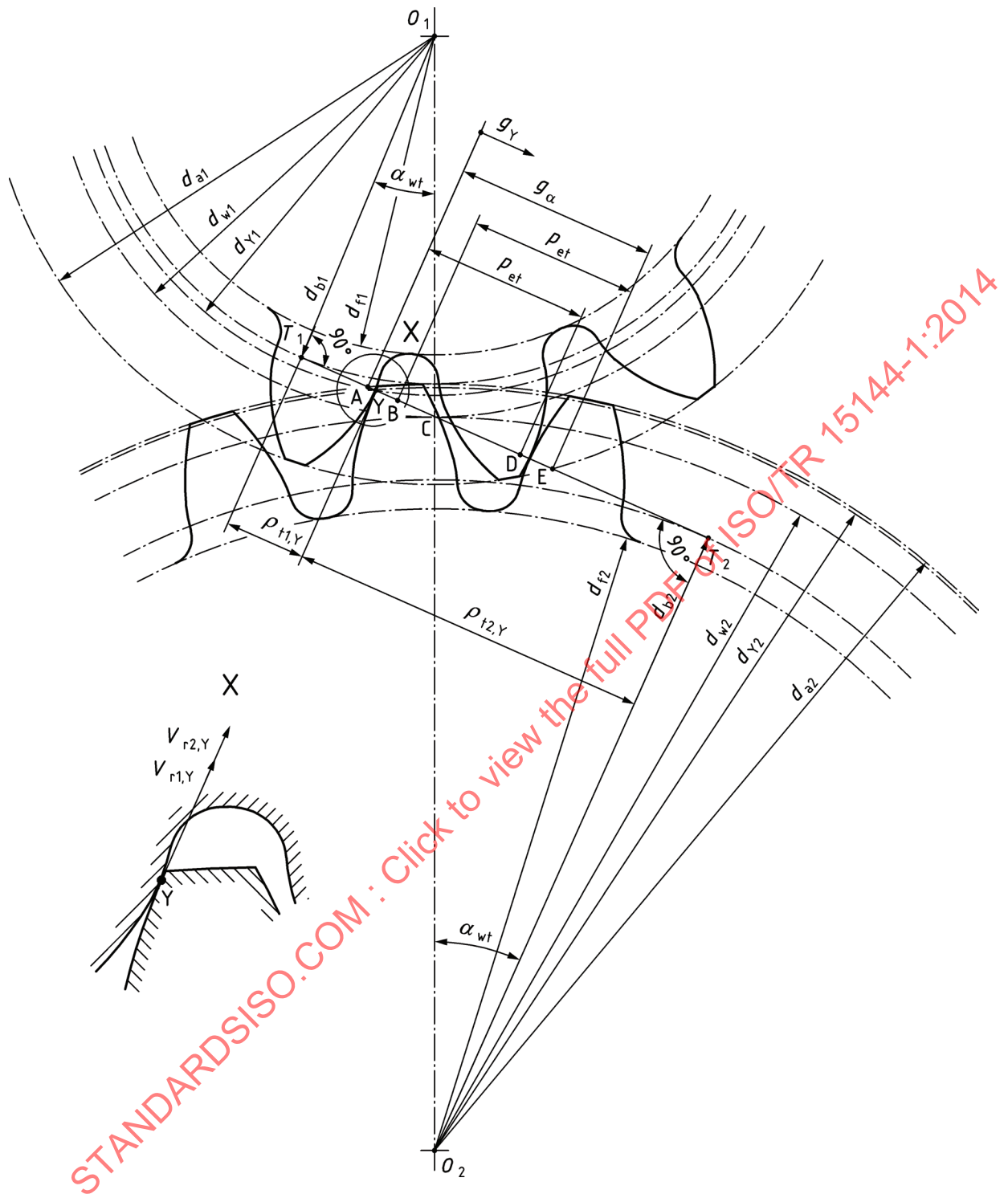


Figure 1 — Definition of contact point Y on the line of action

The Y-circle diameter of pinion dy_1 and wheel dy_2 are dependent on the location of contact point Y on the path of contact gy and can be calculated according to Formula (41) and Formula (42).

$$d_{Y1} = 2 \cdot \sqrt{\frac{{d_{b1}}^2}{4} + \left(\sqrt{\frac{{d_{a1}}^2}{4} - \frac{{d_{b1}}^2}{4}} - g_\alpha + g_Y \right)^2} \quad (41)$$

$$d_{Y2} = 2 \cdot \sqrt{\frac{d_{b2}^2}{4} + \left(\sqrt{\frac{d_{a2}^2}{4} - \frac{d_{b2}^2}{4}} - g_Y \right)^2} \quad (42)$$

where

- d_{a1} is the tip diameter of pinion (see [Figure 1](#));
- d_{a2} is the tip diameter of wheel (see [Figure 1](#));
- d_{b1} is the base diameter of pinion (see [Figure 1](#));
- d_{b2} is the base diameter of wheel (see [Figure 1](#));
- g_Y is the parameter on the path of contact (see [Figure 1](#));
- g_α is the length of path of contact (see [Figure 1](#)).

The transverse radius of relative curvature $\rho_{t,Y}$ can be determined according to Formula (43).

$$\rho_{t,Y} = \frac{\rho_{t1,Y} \cdot \rho_{t2,Y}}{\rho_{t1,Y} + \rho_{t2,Y}} \quad (43)$$

where

$$\rho_{t1,2,Y} = \sqrt{\frac{d_{Y1,2}^2 - d_{b1,2}^2}{4}} \quad (44)$$

- $\rho_{t1,2,Y}$ is the transverse radius of curvature of pinion/wheel at point Y (see [Figure 1](#));
- $d_{b1,2}$ is the base diameter of pinion/wheel (see [Figure 1](#));
- $d_{Y1,2}$ is the Y-circle diameter of pinion/wheel (see above and [Figure 1](#)).

The normal radius of relative curvature $\rho_{n,Y}$ can be calculated according to Formula (45).

$$\rho_{n,Y} = \frac{\rho_{t,Y}}{\cos \beta_b} \quad (45)$$

where

- $\rho_{t,Y}$ is the transverse relative radius of curvature (see above);
- β_b is the base helix angle.

11 Load sharing factor, X_Y

The load sharing factor X_Y accounts for the load sharing of succeeding pairs of meshing teeth. The load sharing factor is presented as a function of the linear parameter g_Y on the path of contact.^[4]

Due to inaccuracies, a preceding pair of meshing teeth can cause an instantaneous increase or decrease of the theoretical load sharing factor, independent of the instantaneous increase or decrease caused by inaccuracies of a succeeding pair of meshing teeth at a later time. The value of X_Y does not exceed 1,0 (for cylindrical gears), which means full transverse single tooth contact. The region of transverse single tooth contact can be extended by an irregularly varying location of a dynamic load.

The load sharing factor X_Y depends on the type of gear transmission and on the profile modification. In case of buttressing of helical teeth (no profile modification), the load sharing factor is combined with a buttressing factor $X_{\text{but},Y}$.^[4]

11.1 Spur gears with unmodified profiles

The load sharing factor for a spur gear with unmodified profile is conventionally supposed to have a discontinuous trapezoidal shape; see [Figure 2](#). However, due to manufacturing inaccuracies, in each path of double contact, the load sharing factor will increase for protruding flanks and decrease for other flanks. The representative load sharing factor is an envelope of possible curves; see [Figure 3](#).

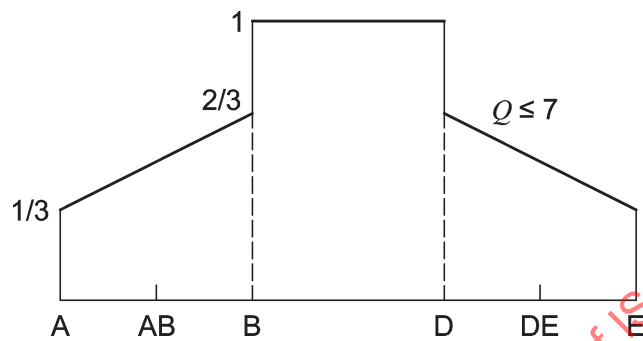


Figure 2 — Load sharing factor for cylindrical spur gears with unmodified profiles and quality grade ≤ 7

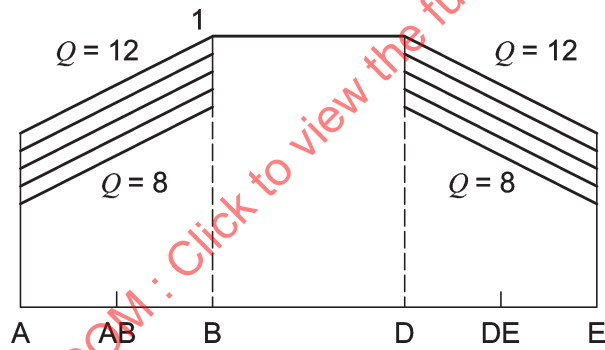


Figure 3 — Load sharing factor for cylindrical spur gears with unmodified profiles and quality grade ≥ 8

$$X_Y = \frac{Q-2}{15} + \frac{1}{3} \cdot \frac{g_Y}{g_B} \quad \text{for } g_A \leq g_Y < g_B \quad (46)$$

$$X_Y = 1,0 \quad \text{for } g_B \leq g_Y \leq g_D \quad (47)$$

$$X_Y = \frac{Q-2}{15} + \frac{1}{3} \cdot \frac{g_a - g_Y}{g_a - g_D} \quad \text{for } g_D < g_Y \leq g_E \quad (48)$$

where

Q is equal to 7 for quality grade ≤ 7 ;

Q is equal to quality grade for grade ≥ 8 .

11.2 Spur gears with profile modification

a) Load sharing factor for cylindrical spur gears with adequate profile modification on driving and driven gear

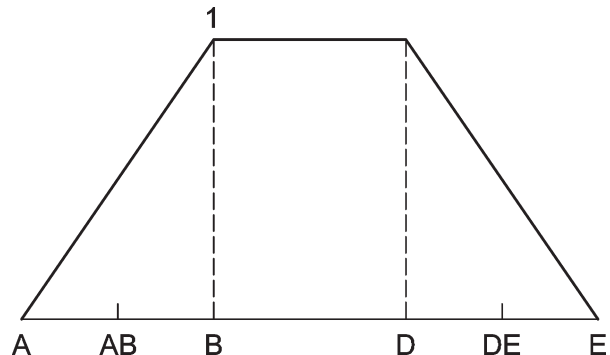


Figure 4 — Load sharing factor for cylindrical spur gears with adequate profile modification

$$X_Y = \frac{g_Y}{g_B} \quad \text{for } g_A \leq g_Y \leq g_B \quad (49)$$

$$X_Y = 1,0 \quad \text{for } g_B < g_Y < g_D \quad (50)$$

$$X_Y = \frac{g_\alpha - g_Y}{g_\alpha - g_D} \quad \text{for } g_D \leq g_Y \leq g_E \quad (51)$$

b) Load sharing factor for cylindrical spur gears with adequate profile modification on the addendum of the driven gear and/or the dedendum of the driving gear

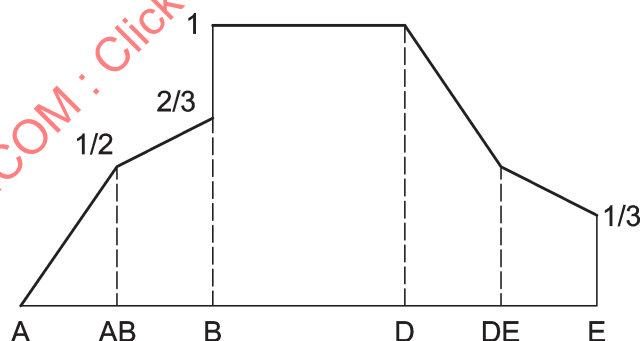


Figure 5 — Load sharing factor for cylindrical spur gears with adequate profile modification on the addendum of the driven gear and/or the dedendum of the driving gear

$$X_Y = \frac{g_Y}{g_B} \quad \text{for } g_A \leq g_Y \leq g_{AB} \quad (52)$$

$$X_Y = \frac{1}{3} + \frac{1}{3} \cdot \frac{g_Y}{g_B} \quad \text{for } g_{AB} < g_Y \leq g_B \quad (53)$$

$$X_Y = 1,0 \quad \text{for } g_B < g_Y < g_D \quad (54)$$

$$X_Y = \frac{g_\alpha - g_Y}{g_\alpha - g_D} \quad \text{for } g_D \leq g_Y \leq g_{DE} \quad (55)$$

$$X_Y = \frac{1}{3} + \frac{1}{3} \cdot \frac{g_\alpha - g_Y}{g_\alpha - g_D} \quad \text{for } g_{DE} < g_Y \leq g_E \quad (56)$$

c) Load sharing factor for cylindrical spur gears with adequate profile modification on the addendum of the driving gear and/ or the dedendum of the driven gear

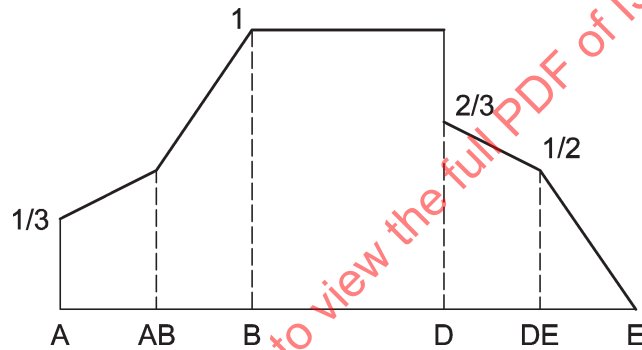


Figure 6 — Load sharing factor for cylindrical spur gears with adequate profile modification on the addendum of the driving gear and/or the dedendum of the driven gear

$$X_Y = \frac{1}{3} + \frac{1}{3} \cdot \frac{g_Y}{g_B} \quad \text{for } g_A \leq g_Y \leq g_{AB} \quad (57)$$

$$X_Y = \frac{g_Y}{g_B} \quad \text{for } g_{AB} < g_Y \leq g_B \quad (58)$$

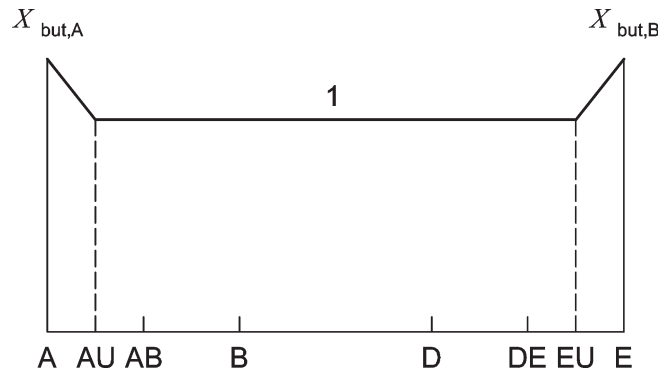
$$X_Y = 1,0 \quad \text{for } g_B < g_Y < g_D \quad (59)$$

$$X_Y = \frac{1}{3} + \frac{1}{3} \cdot \frac{g_\alpha - g_Y}{g_\alpha - g_D} \quad \text{for } g_D \leq g_Y \leq g_{DE} \quad (60)$$

$$X_Y = \frac{g_\alpha - g_Y}{g_\alpha - g_D} \quad \text{for } g_{DE} < g_Y \leq g_E \quad (61)$$

11.3 Buttressing factor, $X_{\text{but},Y}$

Helical gears can have a buttressing effect near the end points A and E of the path of contact, due to the oblique contact lines. This applies to cylindrical helical gears with no profile modification.

Figure 7 — Buttressing factor, $X_{\text{but},Y}$

The buttressing is expressed by means of a factor $X_{\text{but},Y}$; see [Figure 7](#), marked by the following values.

$$g_{\text{AU}} - g_A = g_E - g_{\text{EU}} = 0,2 \text{ mm} \cdot \sin \beta_b \quad (62)$$

where

g_A is equal to 0 mm;

g_E is equal to g_α (see [Figure 1](#))

$$X_{\text{but},A} = X_{\text{but},E} = 1,3 \quad \text{if } \varepsilon_\beta \geq 1,0 \quad (63)$$

$$X_{\text{but},A} = X_{\text{but},E} = 1 + 0,3 \cdot \varepsilon_\beta \quad \text{if } \varepsilon_\beta < 1,0 \quad (64)$$

$$X_{\text{but},\text{AU}} = X_{\text{but},\text{EU}} = 1,0 \quad (65)$$

$$X_{\text{but},Y} = X_{\text{but},A} - \frac{g_Y}{0,2 \text{ mm} \cdot \sin \beta_b} \cdot (X_{\text{but},A} - 1) \quad \text{for } g_A \leq g_Y < g_{\text{AU}} \quad (66)$$

$$X_{\text{but},Y} = 1,0 \quad \text{for } g_{\text{AU}} \leq g_Y \leq g_{\text{EU}} \quad (67)$$

$$X_{\text{but},Y} = X_{\text{but},E} - \frac{g_\alpha - g_Y}{0,2 \text{ mm} \cdot \sin \beta_b} \cdot (X_{\text{but},E} - 1) \quad \text{for } g_{\text{EU}} < g_Y \leq g_E \quad (68)$$

where

ε_β is the overlap ratio.

11.4 Helical gears with $\varepsilon_\alpha < 1$ and unmodified profiles

Helical gears with a contact ratio $\varepsilon_\alpha \geq 1$ and overlap ratio $\varepsilon_\beta < 1$ still have poor single contact of tooth pairs. Hence, they can be treated similar to spur gears, considering the geometry in the transverse plane, as well as the buttressing effect. See [Figure 8](#).

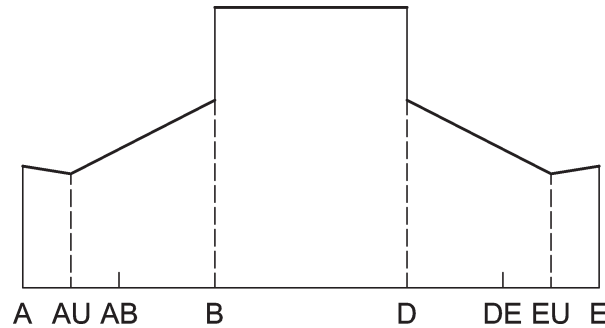


Figure 8 — Load sharing factor for cylindrical helical gears with $\varepsilon_\beta < 1$ and unmodified profiles, including the buttressing effect

The load sharing factor is obtained by multiplying the X_Y in 11.1 with the buttressing factor $X_{\text{but},Y}$ in 11.3.

11.5 Helical gears with $\varepsilon_\beta < 1$ and profile modification

Helical gears with a contact ratio $\varepsilon_\alpha \geq 1$ and overlap ratio $\varepsilon_\beta < 1$ still have poor single contact of tooth pairs. Hence, they can be treated similar to spur gears, considering the geometry in the transverse plane. See [Figure 9](#), [Figure 10](#), and [Figure 11](#).

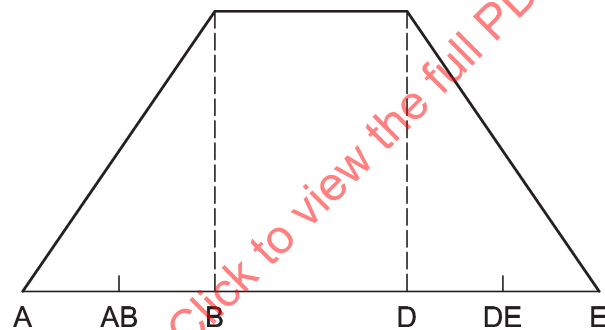


Figure 9 — Load sharing factor for cylindrical helical gears with $\varepsilon_\beta < 1$ and adequate profile modification

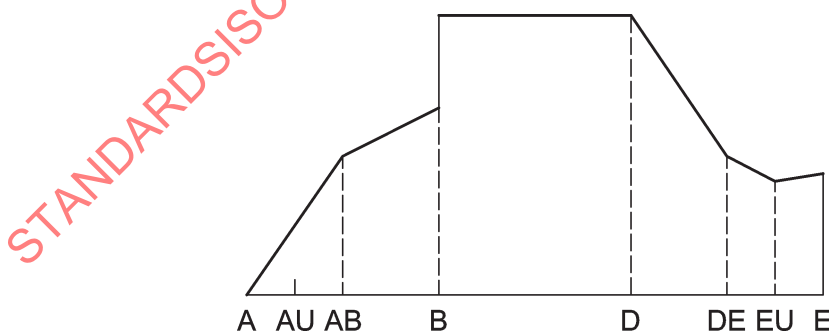


Figure 10 — Load sharing factor for cylindrical helical gears with $\varepsilon_\beta < 1$ and adequate profile modification on the addendum of the driven gear and/or the dedendum of the driving gear

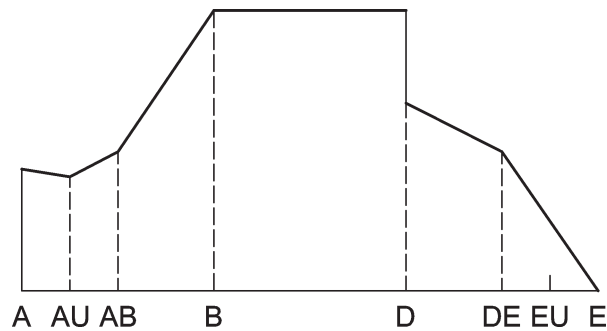


Figure 11 — Load sharing factor for cylindrical helical gears with $\varepsilon_\beta < 1$ and adequate profile modification on the addendum of the driving gear and/or the dedendum of the driven gear

The load sharing factor is obtained by multiplying the X_Y in 11.2 with the buttressing factor $X_{\text{but},Y}$ in 11.3.

11.6 Helical gears with $\varepsilon_\beta \geq 1$ and unmodified profiles

The buttressing effect of local high mesh stiffness at the end of oblique contact lines for helical gears with $\varepsilon_\alpha \geq 1$ and $\varepsilon_\beta \geq 1$, is assumed to act near the ends A and E along the helix teeth over a constant length, which corresponds to a transverse relative distance $0,2 \text{ mm} \cdot \sin\beta_b$; see Figure 12. See also 11.2 and Figure 7.

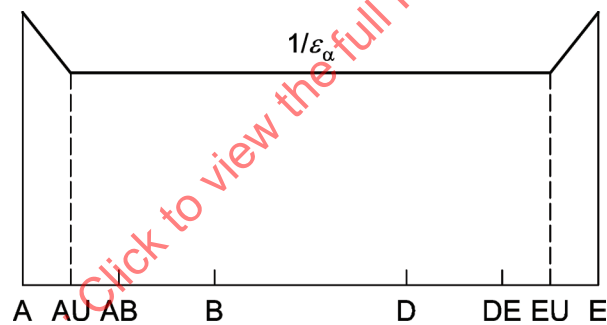


Figure 12 — Load sharing factor for cylindrical helical gears with $\varepsilon_\beta \geq 1$ and unmodified profiles

The load sharing factor is obtained by multiplying the value $1/\varepsilon_\alpha$, representing the mean load, with the buttressing factor $X_{\text{but},Y}$.

$$X_Y = \frac{1}{\varepsilon_\alpha} \cdot X_{\text{but},Y} \quad (69)$$

where

ε_α is the transverse contact ratio.

11.7 Helical gears with $\varepsilon_\beta \geq 1$ and profile modification

Tip relief on the pinion (respectively wheel) reduces X_Y in the range DE-E (respectively A-AB) and increases X_Y in the range AB-DE; see Figures 13, 14, and 15. The extensions of tip relief at both ends

A-AB and DE-E of the path of contact are assumed to be equal and to result in a contact ratio $\varepsilon_\alpha = 1$ for unloaded gears; see [Figure 13](#).

a) Load sharing factor for cylindrical helical gears with $\varepsilon_\beta \geq 1$ and adequate profile modification on driving and driven gear

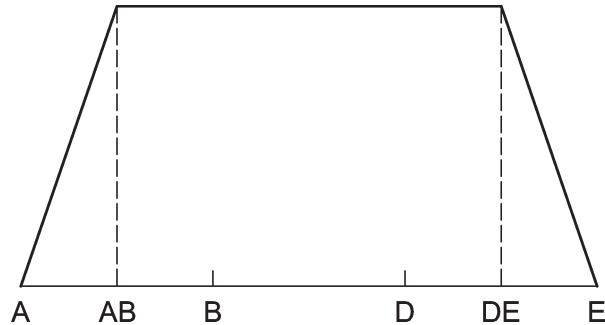


Figure 13 — Load sharing factor for cylindrical helical gears with $\varepsilon_\beta \geq 1$ and adequate profile modification

$$X_Y = \left[\frac{1}{\varepsilon_\alpha} + \frac{(\varepsilon_\alpha - 1)}{\varepsilon_\alpha \cdot (\varepsilon_\alpha + 1)} \right] \cdot \frac{g_Y}{g_{AB}} \quad \text{for } g_A \leq g_Y \leq g_{AB} \quad (70)$$

$$X_Y = \frac{1}{\varepsilon_\alpha} + \frac{(\varepsilon_\alpha - 1)}{\varepsilon_\alpha \cdot (\varepsilon_\alpha + 1)} \quad \text{for } g_{AB} < g_Y \leq g_{DE} \quad (71)$$

$$X_Y = \left[\frac{1}{\varepsilon_\alpha} + \frac{(\varepsilon_\alpha - 1)}{\varepsilon_\alpha \cdot (\varepsilon_\alpha + 1)} \right] \cdot \frac{g_\alpha - g_Y}{g_\alpha - g_{DE}} \quad \text{for } g_{DE} < g_Y \leq g_E \quad (72)$$

b) Load sharing factor for cylindrical helical gears with $\varepsilon_\beta \geq 1$ and adequate profile modification on the addendum of the driven gear and/or the dedendum of the driving gear

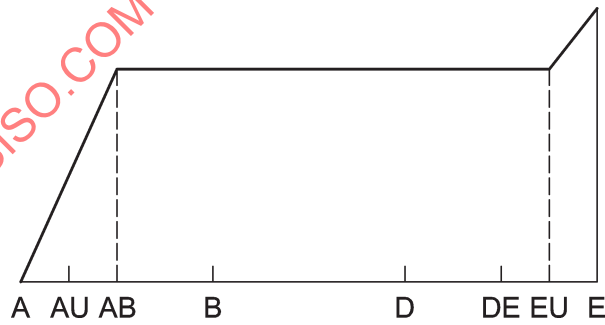


Figure 14 — Load sharing factor for cylindrical helical gears with $\varepsilon_\beta \geq 1$ and adequate profile modification on the addendum of the driven gear and/or the dedendum of the driving gear

$$X_Y = \left[\frac{1}{\varepsilon_\alpha} + \frac{(\varepsilon_\alpha - 1)}{2 \cdot \varepsilon_\alpha \cdot (\varepsilon_\alpha + 1)} \right] \cdot \frac{g_Y}{g_{AB}} \quad \text{for } g_A \leq g_Y \leq g_{AB} \quad (73)$$

$$X_Y = \frac{1}{\varepsilon_\alpha} + \frac{(\varepsilon_\alpha - 1)}{2 \cdot \varepsilon_\alpha \cdot (\varepsilon_\alpha + 1)} \quad \text{for } g_{AB} < g_Y \leq g_{DE} \quad (74)$$

$$X_Y = \left[\frac{1}{\varepsilon_\alpha} + \frac{(\varepsilon_\alpha - 1)}{2 \cdot \varepsilon_\alpha \cdot (\varepsilon_\alpha + 1)} \right] \cdot X_{\text{but},Y} \quad \text{for } g_{DE} < g_Y \leq g_E \quad (75)$$

c) Load sharing factor for cylindrical helical gears with $\varepsilon_\beta \geq 1$ and adequate profile modification on the addendum of the driving gear and/ or the dedendum of the driven gear

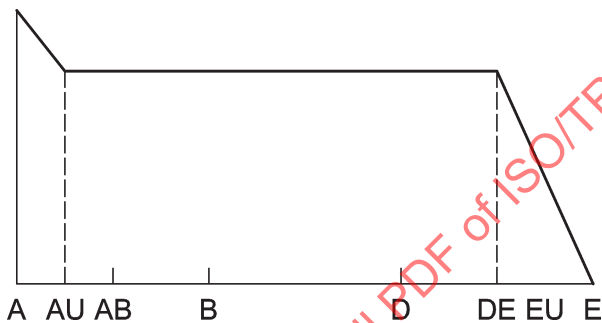


Figure 15 — Load sharing factor for cylindrical helical gears with $\varepsilon_\beta \geq 1$ and adequate profile modification on the addendum of the driving gear and/or the dedendum of the driven gear

$$X_Y = \left[\frac{1}{\varepsilon_\alpha} + \frac{(\varepsilon_\alpha - 1)}{2 \cdot \varepsilon_\alpha \cdot (\varepsilon_\alpha + 1)} \right] \cdot X_{\text{but},Y} \quad \text{for } g_A \leq g_Y \leq g_{AB} \quad (76)$$

$$X_Y = \frac{1}{\varepsilon_\alpha} + \frac{(\varepsilon_\alpha - 1)}{2 \cdot \varepsilon_\alpha \cdot (\varepsilon_\alpha + 1)} \quad \text{for } g_{AB} < g_Y \leq g_{DE} \quad (77)$$

$$X_Y = \left[\frac{1}{\varepsilon_\alpha} + \frac{(\varepsilon_\alpha - 1)}{2 \cdot \varepsilon_\alpha \cdot (\varepsilon_\alpha + 1)} \right] \cdot \frac{g_\alpha - g_Y}{g_\alpha - g_{DE}} \quad \text{for } g_{DE} < g_Y \leq g_E \quad (78)$$

12 Contact temperature, $\theta_{B,Y}$

The local contact temperature $\theta_{B,Y}$ is defined as the sum of bulk temperature θ_M and local flash temperature $\theta_{fl,Y}$. As a result of friction in the teeth mesh, the flash temperature $\theta_{fl,Y}$ varies along the path of contact. Hence, the local flash temperature $\theta_{fl,Y}$ has to be determined for every desired point Y in the field of contact. For simplification, the bulk temperature θ_M is assumed as constant.

$$\theta_{B,Y} = \theta_M + \theta_{fl,Y} \quad (79)$$

where

$\theta_{fl,Y}$ is the local flash temperature (see [Clause 13](#));

θ_M is the bulk temperature (see [Clause 14](#)).

13 Flash temperature, $\theta_{fl,Y}$

The flash temperature $\theta_{fl,Y}$ of the gear flanks is rapidly fluctuating in contact. In every mesh position, different rolling and sliding conditions occur. Furthermore, the local contact load varies along the path of contact. These conditions cause a continuous variation of the flash temperature which can be calculated according to Reference [12] by Formula (80).

$$\theta_{fl,Y} = \frac{\sqrt{\pi}}{2} \cdot \frac{\mu_m \cdot p_{dyn,Y} \cdot 10^6 \cdot |v_{g,Y}|}{B_{M1} \cdot \sqrt{v_{r1,Y}} + B_{M2} \cdot \sqrt{v_{r2,Y}}} \cdot \sqrt{8 \cdot \rho_{n,Y} \cdot \frac{p_{dyn,Y}}{1000 \cdot E_r}} \quad (80)$$

where

$$v_{g,Y} = v_{r1,Y} - v_{r2,Y} \quad (81)$$

$$B_{M1} = \sqrt{\rho_{M1} \cdot c_{M1} \cdot \lambda_{M1}} \quad (82)$$

$$B_{M2} = \sqrt{\rho_{M2} \cdot c_{M2} \cdot \lambda_{M2}} \quad (83)$$

$v_{g,Y}$ is the local sliding velocity;

B_{M1} is the thermal contact coefficient of pinion (see [Table 2](#));

B_{M2} is the thermal contact coefficient of wheel (see [Table 2](#));

μ_m is the mean coefficient of friction (see [14.1](#));

$p_{dyn,Y}$ is the local Hertzian contact stress (see [8.1](#) and [8.2](#));

$v_{r1,Y}$ is the local tangential velocity on pinion (see [7.1](#));

$v_{r2,Y}$ is the local tangential velocity on wheel (see [7.1](#));

$\rho_{n,Y}$ is the local normal radius of relative curvature (see [Clause 10](#));

E_r is the reduced modulus of elasticity (see [6.1](#)).

Table 2 — Material properties of steel

Material	Density ρ_M [kg/m ³]	Specific heat capacity c_M [J/(kg·K)]	Specific heat conductivity λ_M [W/(m·K)]
Steel	7 800	440	45

14 Bulk temperature, θ_M

The bulk temperature θ_M is the equilibrium temperature of the surface of the gear teeth before they enter the contact zone. The bulk temperature θ_M should be measured or calculated by an adequate

method. If this is not possible, θ_M can be approximated according to Formula (84) (compare Reference [9]).

$$\theta_M = \theta_{\text{oil}} + 7400 \cdot \left(\frac{P \cdot \mu_m \cdot H_v}{a \cdot b} \right)^{0,72} \cdot \frac{X_S}{1,2 \cdot X_{C_a}} \quad (84)$$

where

$$P = 2 \cdot \pi \cdot \frac{n_1}{60} \cdot \frac{T_1}{1000} \quad (85)$$

P is the transmitted power;

a is the centre distance;

b is the face width;

θ_{oil} is the lubricant inlet or oil sump temperature;

μ_m is the mean coefficient of friction (see 14.1);

H_v is the load losses factor (see 14.2);

X_{C_a} is the tip relief factor (see 14.3);

X_S is the lubricant factor (see 14.4).

14.1 Mean coefficient of friction, μ_m

The mean coefficient of friction μ_m depends on the gear geometry, the surface roughness, the tangential velocity, the tangential load, and the dynamic viscosity of the lubricant. It can be approximated by Formula (86).

$$\mu_m = 0,045 \cdot \left(\frac{K_A \cdot K_v \cdot K_{H\alpha} \cdot K_{H\beta} \cdot F_{bt} \cdot K_{B\gamma}}{b \cdot v_{\Sigma,C} \cdot \rho_{n,C}} \right)^{0,2} \cdot \left(10^3 \cdot \eta_{\theta\text{oil}} \right)^{-0,05} \cdot X_R \cdot X_L \quad (86)$$

where

$$X_R = 2,2 \cdot \left(\frac{R_a}{\rho_{n,C}} \right)^{0,25} \quad (87)$$

X_R is the roughness factor;

b is the face width;

F_{bt} is the nominal transverse load in plane of action;

K_A is the application factor (according to ISO 6336-1);

$K_{B\gamma}$ is the helical load factor (see below);

$K_{H\alpha}$ is the transverse load factor (according to ISO 6336-1);

$K_{H\beta}$ is the face load factor (according to ISO 6336-1);

K_v is the dynamic factor (according to ISO 6336-1);